

## **ICEC0942, an Orally Bioavailable Selective Inhibitor of CDK7 for Cancer Treatment**

Hetal Patel<sup>1,#</sup>, Manikandan Periyasamy<sup>1,#</sup>, Georgina P. Sava<sup>1</sup>, Alexander Bondke<sup>2</sup>, Brian W. Slafer<sup>2</sup>, Sebastian H. B. Kroll<sup>2</sup>, Marion Barbazanges<sup>2</sup>, Richard Starkey<sup>1</sup>, Silvia Ottaviani<sup>1</sup>, Alison Harrod<sup>1</sup>, Eric O. Aboagye<sup>3</sup>, Laki Buluwela<sup>1</sup>, Matthew J. Fuchter<sup>2</sup>, Anthony, G. M. Barrett<sup>2</sup>, Charles Coombes<sup>1\*</sup>, Simak Ali<sup>1,\*</sup>

<sup>1</sup>Division of cancer, Department of Surgery & Cancer, Imperial College London, Hammersmith Hospital Campus, London W12 0NN, UK

<sup>2</sup>Department of Chemistry, Imperial College London, London SW7 2AZ, UK

<sup>3</sup>Comprehensive Cancer Imaging Centre, Imperial College London, Hammersmith Hospital Campus, London W12 0NN, UK

#These authors should be considered as joint first authors

\*Authors for correspondence: Charles Coombes, Simak Ali, Division of Cancer, Department of Surgery & Cancer, Imperial College London, Hammersmith Hospital Campus, London W12 0NN, UK

Email: c.coombes@imperial.ac.uk; [simak.ali@imperial.ac.uk](mailto:simak.ali@imperial.ac.uk)

**Running title:** ICEC0942, a CDK7 inhibitor for Cancer Therapy

**Keywords:** Transcription, cell cycle, cyclin-dependent kinase, CDK7, estrogen receptor, endocrine therapy

**Abbreviations:** cyclin-dependent kinase (CDK); C-terminal domain (CTD); RNA polymerase II (PolII); Estrogen receptor (ER); bromodomain and extra-terminal proteins (BET); positive transcription elongation factor (P-TEFb), Androgen receptor (AR); absorption, distribution, metabolism and excretion (ADME); pharmacokinetics (PK); structure activity relationships (SAR); phosphate buffered saline (PBS); dimethylsulfoxide (DMSO); peripheral blood mononuclear cells (PBMC); immunohistochemistry (IHC); Dulbecco's Modified

Eagle Medium (DMEM); fetal calf serum (FCS). sulforhodamine B (SRB); Propidium iodide (PI); Hank's Balanced Salt Solution (HBSS); Liquid chromatography tandem mass spectrometry (LC-MS/MS).

**Disclosure of potential conflict of interest:** The authors are inventors on a patent on ICEC0942 that is owned by Imperial College London. S. Ali has acted as a consultant for Carrick Therapeutics, plc. ICEC0942 is now under clinical development by Carrick Therapeutics under the name CT7001.

## Abstract

Recent reports indicate that some cancer types are especially sensitive to transcription inhibition, suggesting that targeting the transcriptional machinery provides new approaches to cancer treatment. Cyclin-dependent kinase (CDK)7 is necessary for transcription, and acts by phosphorylating the C-terminal domain (CTD) of RNA polymerase II (PolII) to enable transcription initiation. CDK7 additionally regulates the activities of a number of transcription factors, including Estrogen receptor- $\alpha$  (ER). Here we describe a new, orally bioavailable CDK7 inhibitor, ICEC0942. It selectively inhibits CDK7, with an  $IC_{50}$  of 40nM;  $IC_{50}$  values for CDK1, CDK2, CDK5 and CDK9 were 45-, 15-, 230- and 30-fold higher. *In vitro* studies show that a wide range of cancer types are sensitive to CDK7 inhibition with  $GI_{50}$  values ranging between 0.2-0.3  $\mu$ M. In xenografts of both breast and colorectal cancers, the drug has substantial anti-tumor effects. Additionally, combination therapy with tamoxifen showed complete growth arrest of ER-positive tumor xenografts. Our findings reveal that CDK7 inhibition provides a new approach, especially for ER-positive breast cancer and identify ICEC0942 as a prototype drug with potential utility as a single agent or in combination with hormone therapies for breast cancer. ICEC0942 may also be effective in other cancers that display characteristics of transcription factor addiction, such as acute leukaemia, and small-cell lung cancer.

## Introduction

Despite considerable evidence for dysregulation of transcription in cancer, inhibition of transcription has traditionally been viewed as being likely to suffer from toxicity, due to its requirement in normal tissues and consequent presumed lack of selective action in cancer cells. However, studies highlighting the potential of inhibiting bromodomain and extra-terminal proteins (BET) proteins that interact with the positive transcription elongation factor (P-TEFb; comprised of the CDK9 and cyclin T1 heterodimer) (1-3), show promise for cancers dependent on transcriptional drivers, such as c-Myc, the androgen receptor (AR) and ER (4-6). Our group, through the development of BS-181, has demonstrated the marked sensitivity of many cancer types to selective CDK7 inhibition (7). More recently, a covalent CDK7 inhibitor, THZ1, has also been found to selectively inhibit growth of cancer cells at doses at which normal cells are insensitive (8-11). The cancer selectivity in the latter studies appears to be due to the particular sensitivity of genes encoding key transcriptional drivers to inhibition of PolII activity, such as RUNX1 (T-cell acute lymphoblastic leukaemia) (8) and N-myc (neuroblastoma) (9).

CDK7 is a component of TFIIH, the basal transcription factor that is recruited to transcription start sites alongside PolII, and which phosphorylates serine-5 in the C-terminal domain (CTD) repeat region of PolII, to facilitate transcription initiation. CDK7 also phosphorylates CDK9 (P-TEFb), which in turn is responsible for phosphorylation of the PolII CTD at serine-2. PolII and CDK9 phosphorylation by CDK7 are required for transcription by PolII (12). In addition, CDK7 directly regulates the activities of several transcription factors, including nuclear receptors RAR $\alpha$ , RAR $\gamma$ , AR and ER (13-17), as well as p53 (18,19). For nuclear receptors, phosphorylation of CDK7 target sites in the N-terminal transcription activation functions is frequently mediated by ligand-dependent recruitment of TFIIH to the C-terminal hormone binding domain. CDK7 targeted phosphorylation of these receptors is required for full activity and directed ubiquitination and proteasomal degradation critical for the

cyclical recruitment of these transcription factors to gene promoters (15,16,20,21). The role of TFIIH/CDK7 in regulating the activities of specific transcription regulators, further highlights the potential for cancer selective action of CDK7 inhibitors, for example in breast and prostate cancer, for which ER and AR respectively, are critical drivers.

In addition to its function in transcription, CDK7 directs cell cycle progression by phosphorylating CDK1, 2, 4 and 6 (22,23). Deregulation of cell cycle CDKs, affected by, for example, cyclin D1 over-expression or silencing of CDK inhibitor expression, is a common feature in cancer (24). This may mean that cancer cells are more sensitive than normal cells, to inhibition of cell cycle CDK activities. Indeed, several inhibitors of cell cycle CDKs have entered advanced clinical trial settings, the most prominent of which, the CDK4/6 inhibitor palbociclib, shows promise, although there is significant toxicity, especially neutropenia, gastro-intestinal disorders and alopecia, associated with its use in the combination setting with anti-estrogens or aromatase inhibitors in ER-positive breast cancer (25,26).

BS-181 is a selective small molecule inhibitor of CDK7, which inhibits cancer cell growth *in vitro* and *in vivo* (7). However, absorption, distribution, metabolism and excretion (ADME) and pharmacokinetic (PK) assays highlighted poor cell permeability and oral bioavailability, prompting us to develop BS-181 analogues that maintain CDK7 selectivity, but have improved drug-like properties. We reasoned that oral bioavailability was of importance in view of the potential need for co-administration with oral anti-endocrine agents, given over considerable periods of time in the adjuvant therapy of breast cancer. Iterative compound design using *in silico* modelling of BS-181 and the structurally related orally bioavailable CDK1/2/5/7/9 inhibitor BS-194 (27) in the CDK7 X-ray crystallographic structure, testing potency and CDK7 selectivity using *in vitro* and cell-based assays and *in vivo* PK, allowed development of structure activity relationships (SAR) for a larger series of compounds. These approaches have yielded a new CDK7 non-covalent ATP competitive inhibitor, ICEC0942, with good ADME/PK properties and significant oral bioavailability. We show that ICEC0942 inhibits the growth of

multiple cancer cell lines and is effective as a single agent or in combination with endocrine therapies. Our results therefore provide a rationale for the use of CDK7 inhibitors in the treatment of cancer, especially ER-positive breast cancer.

## Material and Methods

**Chemicals.** Synthesis of ICEC0942 has been described (28). FT-NMR and high-resolution mass spectrometry were used to confirm structure and material at a purity of >99% (by HPLC) was used. ICEC0942 was solubilised in DMSO at a concentration of 10 mM. Tamoxifen (T5648), 4-hydroxytamoxifen (H7904) and fulvestrant (I4409) were purchased from Sigma-Aldrich (Dorset, UK).

***In vitro* kinase assays.** Activities of purified CDK1/cycA1, CDK2/cycA1, CDK4/cycD1, CDK5/p35NCK and CDK6/cycD1 from Proqinase GmbH (Freiburg Germany), were assayed using the Rb-CTF peptide (Proqinase GmbH cat number: 0040-0000-6), according to manufacturer's protocols. A peptide having the sequence N-YSPTSPSYSPTSPSYSPTSPS-C (PolII CTD) was used as the substrate for CDK7/cycH/MAT1 and CDK9/cycT1 (Proqinase GmbH). Kinase inhibition was evaluated by determining ATP remaining at the end of the kinase reaction using a luciferase assay (PKLight assay, Cambrex), as described (27). Screening of a 117 kinase panel with 10  $\mu$ M ICEC0942 was performed by the International Centre for Kinase Profiling (<http://www.kinase-screen.mrc.ac.uk/>).

**Cell proliferation.** Cell lines were purchased from the American Type Culture Collection (ATCC: [www.lgcstandards-atcc.org](http://www.lgcstandards-atcc.org)) as frozen stocks and were cultured in Dulbecco's Modified Eagle Medium (DMEM) supplemented with 10% fetal calf serum (FCS). Once established in the laboratory, the authenticity of the lines was further confirmed using Short Tandem Repeat (STR) analysis as described in 2012 in ANSI Standard (ASN-0002) Authentication of Human Cell Lines: Standardization of STR Profiling by the ATCC Standards Development Organization (SDO) (see ref. (29)). Cell stocks were not used 20 passages beyond initial thawing. Cell cultures were routinely tested for Mycoplasma infection by assay of culture supernatants, and found to be negative, using the MycoAlert Mycoplasma detection kit (Lonza, UK). Cell numbers were assessed using the sulforhodamine B (SRB) assay (30).

**Immunoblotting.** Whole cell lysates were prepared in RIPA buffer (Sigma-Aldrich, UK), supplemented with protease and phosphatase inhibitor cocktails (Roche, UK), as previously described (7).

**Antibodies.**  $\beta$ -actin (ab2380), CDK7 P-Thr170 (ab59987), CDK7 (ab9516), cyclin H (ab54903), PolII P-Ser2 (ab5095), PolII P-Ser5 (ab5131), PolII (ab817), RB P-Thr821 (ab4787), CTSD (ab6313), MYC (ab32), CCND1 (ab16663) and PGR (ab821) were purchased from Abcam plc, UK. ER P-Ser118 (sc12915), MAT1 (sc135981) and RB (sc-50) were supplied by Santa Cruz Biotechnology Inc. (Germany). Cell Signaling Technology Inc. (USA) provided CDK1 (9112), CDK1 P-Thr161 (9114), CDK2 (2546), PARP1 (9542), RB P-Ser780 (9307), P-Ser795 (9301), P-Ser807/811 (9308), CHK2 (2662), CHK2 P-Thr68 (2661) and CHK2 P-Ser516 (2669) antibodies. The ER (VPE613), PolII P-Ser7 (61087), CDK2 P-Thr160 (PAB0438) and Ki-67 (Mib-1) antibodies were obtained from Vector Laboratories, Active Motif, Abnova and DAKO respectively.

**Flow cytometry.** Cell cycle analysis was carried out 24 hours following addition of ICEC0942 to  $4 \times 10^5$  cells, as described (27). Propidium iodide (PI) stained cells were processed using the RXP cytomics software on a Beckman FACS Canto (Beckman Coulter, UK) and analyzed using Flow Jo (Tree Star Inc., CA). For apoptosis, Annexin V and PI labelling and flow cytometry was undertaken exactly as previously described (7). Enrichment for cells in G0/G1 was achieved by culturing  $1 \times 10^5$  cells in serum-free DMEM for 48 hours. For enrichment of cells in the S-phase, a double thymidine block was used, in which 2 mM thymidine was added to cells in DMEM/10% FCS, for 18 hours, followed by washing in Hank's Balanced Salt Solution (HBSS), and addition of 2 mM thymidine in DMEM/10% FCS, for a further 18 hours. For arrest in G2/M, cells were cultured in DMEM/10%FCS containing 2 mM thymidine for 24 hours, washing in HBSS and culturing in medium containing 100 ng/ml nocodazole for 12 hours. At the end of synchronization steps, cells were washed with HBSS and culturing in medium supplemented with ICEC0942 for



0-48 hours.

**Caspase 3/7 Assay.** Cells were plated in optical quality 96 well-plates and treated for 24 hours with the indicated concentration of ICEC0942 or DMSO control. The Caspase-Glo 3/7 Assay (Promega, UK) was used according to manufacturer's instructions.

**Tumour xenografts.** All experiments were done by licensed investigators in accordance with the UK Home Office Guidance on the Operation of the Animal (Scientific Procedures) Act 1986 (HMSO, London, UK, 1990) and within guidelines set out by the UK National Cancer Research Institute Committee on Welfare of Animals in Cancer Research (31). Tumour xenograft studies were carried out as described previously (7,27), following injection of  $5 \times 10^6$  cells s.c. in a volume  $\leq 0.1$  ml, into the flanks of seven-week old female nu/nu-BALB/c athymic nude mice (Harlan Olac, UK). For MCF7 xenografts, a 0.72 mg  $17\beta$ -estradiol 60 day release pellet (Innovative Research of America) was implanted s.c., 24 hours before inoculation with cells. Animals were randomized and treated daily by oral gavage with ICEC0942, prepared in 10% DMSO/PBS (vehicle), once tumors size reached 100-200 mm<sup>3</sup>. Tamoxifen (100  $\mu$ g/mouse) was administered orally. Animals were weighed daily and tumors measured twice weekly. Tumor volumes were calculated using the formula  $1/2[\text{length (mm)}] \times [\text{width (mm)}]^2$ .

At the end of the study, tumors were divided in half for paraffin embedding or storage at -70C. Protein lysates were prepared by homogenization of frozen tumors in RIPA buffer. Animal blood was acquired by cardiac puncture. For blood biochemistry, blood was allowed to clot at room temperature, centrifuged and 200  $\mu$ l of serum analysed. Blood processing for cell counts and PolIII phosphorylation assessment of peripheral blood mononuclear cells (PBMC), has been described (27). Blood biochemistry and cell counts were undertaken by the Clinical Biochemistry and the Haematology services at St Mary's Hospital.

**Immunohistochemistry (IHC).** IHC was performed as described previously (27), using antibodies listed above. Images were acquired using the Automated Cellular Imaging System (ACIS) (Carl Zeiss Ltd., Welwyn Garden City, UK); >1000 cells were scored per section for 3 tumors.

**Absorption, Distribution, Metabolism, Elimination and Toxicity (ADME-Tox) and Pharmacokinetic Studies.** *In vitro* ADME assays and *in vivo* PK analysis were performed by Cyprotex (Macclesfield, UK) using described methods (<http://www.cyprotex.com/admepk/>). Liquid chromatography tandem mass spectrometry (LC-MS/MS) was used for quantitative detection of ICEC0942.

**Statistical analyses.** For statistical analysis, pairwise comparisons were performed using the Student's t-test in Graphpad Prism v7.0. Linear regression was used for comparison of tumor xenograft inhibition data. Multiple comparison tests where more than two treatment groups were compared, was carried out using one-way ANOVA analysis of the slopes of linear regression lines.

## Results

### ICEC0942 is a selective inhibitor of CDK7

ICEC0942 inhibited CDK7 activity *in vitro* with an  $IC_{50}$  of 40 nM (Fig. 1A, B, Supplementary Fig. S1A).  $IC_{50}$  values for CDK1, CDK2, CDK5 and CDK9 were 45-, 15-, 230- and 30-fold higher, whilst CDK4 and CDK6 were not substantially inhibited by ICEC0942, demonstrating CDK7 selectivity. ICEC0942 has a very similar spectrum of activity to our previously described, selective CDK7 inhibitor, BS-181 (7). Moreover, screening of 117 kinases representing different kinase classes confirmed CDK7 selectivity (Supplementary Fig. S1B). ERK8, STK33, CHK2, CLK2 and PHK were

inhibited at this high concentration (10  $\mu\text{M}$ ) of ICEC0942, but to an extent similar to the level of inhibition observed for CDK2.

ICEC0942 inhibited the growth of breast cancer cell lines with  $\text{GI}_{50}$  values between 0.2-0.3  $\mu\text{M}$  (Fig. 1C). The non-tumorigenic breast epithelial cell line MCF10A and primary human mammary epithelial cells (HMEC) were at least 2- and 3.8 times less sensitive, respectively, to ICEC0942 than breast cancer cell lines, suggestive of a greater sensitivity of breast cancer cell lines to CDK7 inhibition. To extend the analysis to a more extensive set of cancer types, ICEC0942 was submitted to the National Cancer Institute's Division of Cancer Treatment and Diagnosis (<http://dtp.nci.nih.gov/branches/btb/ivclsp.html>) *in vitro* screen of 60 human cell lines representative of diverse cancer types. ICEC0942 inhibited all 60 cancer cell lines, with median  $\text{GI}_{50} = 0.25 \mu\text{M}$  (Fig. 1D). These results indicate that ICEC0942 inhibits cancer cell growth with  $\text{GI}_{50}$  values consistent with specific inhibition of CDK7.

### **ICEC0942 inhibits phosphorylation of CDK7 substrates and promotes cell cycle arrest and apoptosis**

Phosphorylation of the PolIII CTD heptapeptide repeat at serines 2, 5 and 7 is required for transcription initiation and PolIII processon (12). We investigated the effect of CDK7 inhibition in HCT116 cells, as they were particularly sensitive to ICEC0942 (Fig. 1D). PolIII CTD phosphorylation was inhibited by ICEC0942 in a dose and time dependent manner in HCT116 colon cancer cells (Figure 2A). ICEC0942 did not affect levels of CDK7, its cyclin partner (cyclin H) or the accessory protein MAT1. Nor was CDK7 phosphorylation in the T-loop (Thr170) altered by ICEC0942. CDK1 and CDK2 phosphorylation at Thr161 and Thr160, respectively, is mediated by CDK7 and ICEC0942 inhibited phosphorylation of these sites. Phosphorylation of retinoblastoma (Rb) (32), was also reduced, further confirming that ICEC0942 inhibits the activities of CDK2/4/6. ICEC0942 similarly inhibited PolIII, CDK1, CDK2 and RB phosphorylation in the MCF7 breast cancer cell line in a time and dose-

dependent manner (Supplementary Fig. S2A). Interestingly, treatment with 10  $\mu$ M ICEC0942 reduced PolII levels in both cell lines. Reduction in levels was not evident for CDK7, its associated proteins cyclin H, MAT1 or for other CDK7 substrates. Whether PolII loss is due to inhibition of additional kinases at this high concentration of ICEC0942 is unclear, but it should be noted that at these high concentrations ICEC0942 can directly inhibit CDK9 (Figure 1B), which phosphorylates PolII and factors controlling transcription elongation. Phosphorylation of serine 118 (Ser118), the site in ER targeted by CDK7 (15), was also inhibited in MCF7 cells (Supplementary Fig. S2A).

Since ICEC0942 inhibited CDK7-mediated phosphorylation of CDK1 and CDK2, we investigated its effects on apoptosis and the cell cycle. Treatment with ICEC0942 for 24 hours induced caspase 3/7 and demonstrated PARP cleavage, both indicators of programmed cell death (Fig. 2B-D; Supplementary Figure S2B). Further, cell cycle analysis of ICEC0942-treated asynchronous HCT116 cells showed accumulation of cells in G2/M (Figure 2E). Enrichment of cells in G2/M was also observed for asynchronous MCF7 cells (Supplementary Fig. S2C). To determine if ICEC0942 could block cells in other phases of the cell cycle, MCF7 cells were treated with thymidine-nocodazole to induce G2/M arrest (Supplementary Fig. S3A, B). Release from G2/M arrest by washing cells and replenishing with fresh medium, in the presence or absence of ICEC0942 showed that the cells remained blocked in G2/M, even at 48 hours following ICEC0942 addition. The reduced recovery from G2/M block was evident for 1.0  $\mu$ M ICEC0942, but was particularly strong at 10 and 25  $\mu$ M (Fig. 2E; Supplementary Figure S3B). Interestingly, ICEC0942 also blocked release from G1 and slowed release from S-phase arrest, consistent with reports demonstrating that CDK7 is required for CDK2 (G1/S) and CDK4/6 (G1) activities in cancer cells (23,33).

Although G2/M arrest has been reported for THZ1 (8), screening of 117 kinase showed that ICEC0942 can inhibit CHK2 at high concentrations (Supplementary Fig. S1B). As CHK2 activation by DNA damage arrests cells in G1/S and G2/M (34), we determined if ICEC0942 inhibits CHK2 activation. In the absence of DNA damage conditions, there was only low level CHK2

phosphorylation in MCF7 cells, although phosphorylation of the ATM-directed Thr68 was stimulated by 10  $\mu$ M ICEC0942 (Supplementary Fig. S3C). Phosphorylation of Ser516, a CHK2 autophosphorylation site that is indicative of CHK2 activity (eg see ref (35)), was also not greatly affected with ICEC0942 treatment. To investigate the effect of ICEC0942 on CHK2 activity, MCF7 cells were treated with etoposide, which promotes ATM-directed CHK2 phosphorylation at Thr68. Etoposide stimulated Thr68 phosphorylation, which was not affected by ICEC0942 (Supplementary Fig. S3D). P-Ser516 levels were unaffected at concentrations of  $\geq 1.0$   $\mu$ M ICEC0942, with a small reduction in P-Ser516 with 2  $\mu$ M ICEC0942 and strong inhibition at higher ICEC0942 concentrations, suggesting that CHK2 inhibition could be involved in cell cycle arrest at high concentrations of ICEC0942.

### **ICEC0942 is an orally bioavailable small molecule inhibitor of CDK7**

ADME assays were consistent with acceptable or excellent properties for aqueous solubility, plasma protein binding (PPB) and absence of hERG liability (Supplementary Fig. S4A-C). To investigate pharmacokinetics, CD1 male mice were treated intravenously (IV), subcutaneously (SC) or by oral gavage (PO) with 10 mg/kg ICEC0942 (Supplementary Fig. S4D). In plasma, ICEC0942 levels declined in a bi-phasic manner (Supplementary Fig. S4E), indicating rapid distribution into tissues. *In vitro* human PPB was moderate to high at 90.8% (fraction unbound ( $f_u$ ) = 9.2%) (Supplementary Fig. S4A). However, Volume of Distribution (Vd), at 13.0 L/kg, was large (total body water in mice 0.6 L/kg) (Supplementary Fig. S4F), indicating that PPB would not be “restrictive” in distribution for this compound. In keeping with the high Vd, drug levels in the tumors and in liver, were found to be maintained at high levels compared to blood (see below). A  $\log D_{7.4}$  of 1.88 (Supplementary Fig S4A) indicated an approximate 100-fold preference for the compound for the organic over the aqueous phase, predicting tissue distribution of ICEC0942.

Following IV administration of ICEC0942 at 10 mg/kg in male CD1 mice  $Cl_{\text{plasma}}$  was calculated at 78 ml.min/kg. A blood/plasma ratio (BI/PI) of 1.81

was observed, which indicates a  $Cl_{\text{blood}}$  of 43 mL.min/kg, about 48% of hepatic blood flow in the mouse. ICEC0942 has a half-life of 1.9 hrs, a moderate half-life in this species. Metabolite analysis of plasma recovered 2 and 4 hours following a single PO administration (100 mg/kg), showed that only a small proportion (13.5%) of ICEC0942 was metabolized, to give oxidation or dehydrogenation products (Supplementary Figure S4G). Thus, the greater proportion of the parental CDK7 inhibitor remains unmetabolised, even at 4 hours.

Comparing exposure ( $AUC_t$ ) after single PO and IV administration at 10 mg/kg, oral bioavailability (F%) was calculated at 30% (Supplementary Figure S4D, F). Median  $T_{\text{max}}$  for PO administration was 2 hours and was unaffected by increasing dose (Supplementary Figure S4H-K). Over this dose range,  $C_{\text{max}}$  was linearly associated with dose, as was the total exposure over time ( $AUC_t$ ). Taken together, these findings indicate that ICEC0942 can be developed as an oral drug.

### **Oral administration of ICEC0942 inhibits tumor growth *in vivo***

We previously showed that immunostaining and flow cytometry of PBMCs allows determination of CDK7 inhibitor activity *in vivo* (27). Single dose PO administration of ICEC0942, resulted in a concentration-dependent reduction in PolII phosphorylation within 6 hours (Supplementary Fig. S5), with no change in total PolII levels. To assess tumor growth inhibition, we treated established MCF7 tumor xenografts with 100 mg/kg/day ICEC0942 PO. At day 14, tumor growth was inhibited by 60% ( $p=0.0001$ ,  $n=12$ ), accompanied by highly significant reductions in PolII Ser2 and Ser5 phosphorylation in PBMCs and in tumors (Figure 3A-C), consistent with distribution of the drug to tumors (see below). ER Ser118 phosphorylation was also reduced in ICEC0942 treated tumours, as was phosphorylation of CDK1 and CDK2 (Figure 3D).

We also treated nude mice with established HCT116 tumor xenografts daily with 100mg/kg of ICEC0942. Tumor growth was inhibited by 60% ( $p < 0.0001$ ,  $n = 15$ ) by day 13, without significant loss in animal weight (Fig. 4A, B). Resected tumors showed substantial reduction in P-Ser2 and P-Ser5 (Fig. 4C), accompanied by only a slight reduction in total PolII. P-Ser2 and P-Ser5 levels were reduced by 40% and 60%, respectively, in PBMCs collected at the end of the experiment (Figure 4D). ICEC0942 appeared to be well-tolerated, as treated mice showed no significant weight loss and blood biochemistry was normal (Fig. 4E). The only observable adverse event was reduced lymphocyte counts in ICEC0942 treated animals (Fig. 4F).

### **ICEC0942 *in vivo* Pharmacokinetics in Tumor-Bearing Mice**

In both MCF7 and HCT116 tumor xenografts, ICEC0942 plasma concentrations followed similar patterns; thus, in HCT116-bearing mice, at 6 h post initial administration, ICEC0942 concentrations in plasma were almost twice as high for the 100 mg/kg, compared with a 50 mg/kg dose (Supplementary Fig. S6A). There was appreciable accumulation of ICEC0942 in tumors 6-hours post administration, although the tumor levels of ICEC0942 were only 1.36-fold higher for 100 mg/kg versus 50 mg/kg.

We also noted that, plasma concentrations of ICEC0942 after 13 days of daily ICEC0942 administration (100 mg/kg) were approximately twice as high as levels at first administration, possibly due to inhibition of CYP2D6, CYP3A3 and CYP2B6 (Supplementary Fig. S4C). This was not predicted from the plasma kinetics of ICEC0942 in CD1 mice, which indicated a half-life of 1.9 h (Supplementary Fig. S4D). However, it is notable that the plasma concentrations of ICEC0942 were similar in female nu/nu BALB/c mice bearing HCT116 xenografts tumors and in non-tumor bearing male CD1 animals, following a single PO administration of ICEC0942 (Supplementary Fig. S6B) and so are unlikely to reflect mouse strain differences. Following PO administration of 100 mg/kg ICEC0942 in nude mice, mean plasma  $C_{max}$  (1.6  $\mu\text{g/mL}$  (3.7  $\mu\text{M}$ )) was reached at 1 hour (Supplementary Fig. S6B).

Thereafter, ICEC0942 levels decreased, being below the limit of detection by 48 hours. A similar plasma profile was obtained for male CD1 animals. ICEC0942 levels in tumors lagged behind plasma levels; thus, the mean maximum concentration (0.93  $\mu\text{g/mL}$  (2.1  $\mu\text{M}$ )) was observed at 6 hours. Levels subsequently decreased 3.7-fold between 6 and 12 h (0.25  $\mu\text{g/mL}$  (0.6  $\mu\text{M}$ )), but remained at this level throughout the remainder of the time course, indicating retention of the compound in the tumor tissue. This observation is the likely explanation for the greater than expected levels of ICEC0942 in tumor tissue upon repeat dosing and may explain the elevated levels of drug in plasma achieved at the end of the repeat dosing.

### **Co-Administration of CDK7 Inhibitors with Endocrine Therapy**

ER is the key transcriptional driver in breast cancer; its activity requires estrogen binding and is regulated by phosphorylation (36). In agreement with our previous studies which showed that estrogen binding promotes TFIIH recruitment to the ER ligand binding domain, to facilitate phosphorylation of Ser118 by CDK7 (15), ICEC0942 inhibited Ser118 phosphorylation in MCF7 cells in culture and in tumor xenografts (Fig 3D, Supplementary Fig S2A), indicating that ICEC0942 inhibits ER activity. These results prompted us to investigate whether ICEC0942 might be effective in combination treatment with anti-estrogens. Over the course of a 9-day growth assay, 1.0  $\mu\text{M}$  ICEC0942 completely inhibited MCF7 growth. For 0.1  $\mu\text{M}$  ICEC0942, MCF7 growth was inhibited by about 50%, consistent with its  $\text{GI}_{50}$  (Fig. 5A, Supplementary Fig. S7A-B). At this dose of ICEC0942, co-treatment with tamoxifen resulted in considerably greater growth inhibition than was achieved for the single agents. A similar combinatorial growth inhibition was achieved for ICEC0942 with fulvestrant. At these concentrations, tamoxifen did not affect PolII phosphorylation, nor was the ICEC0942-dependent inhibition of PolII phosphorylation greater in the presence of tamoxifen (Fig. 5B). ICEC0942 did inhibit the tamoxifen stimulation of ER phosphorylation at Ser118. Inhibition of ER target genes PGR and CTSD was greater for ICEC0942 than for tamoxifen. Interestingly, at low concentrations (0.1  $\mu\text{M}$ )



ICEC0942, reduction in levels of the ER regulated MYC and CCND1, was greater for the ICEC0942 and tamoxifen combination than for either agent alone, suggestive of a combinatorial effect of the two drugs for a subset of ER regulated genes. At this concentration (0.1  $\mu$ M) ICEC0942, there was an increase in the proportion of cells in G1, but no apparent effect of the combination on apoptosis (Fig. 5C, D).

To test the combined action of hormone therapy and ICEC0942 *in vivo*, we administered 50 mg/kg/day ICEC0942 and 100  $\mu$ g/day tamoxifen to nude mice bearing MCF7 xenograft tumors. This dose of tamoxifen was based on previous studies (37). Since treatment with 100 mg/kg/day ICEC0942 almost completely blocked MCF7 xenograft tumor growth (Fig. 3), we decided to use a lower dose of ICEC0942 was used to allow a combination effect to be readily observable. Note that at a dose of 50 mg/kg, reductions in PolIII phosphorylation were similar to those obtained with 100 mg/kg administration (Supplementary Fig. S5). Co-administration of ICEC0942 and tamoxifen resulted in substantially greater tumor growth inhibition *in vivo* than was observed for either agent alone (Fig. 5E). We quantified the Ki-67 proliferation marker for all treated tumors recovered at the end of the study. This showed significant reduction in Ki-67 ( $p < 0.05$ ), but the reduction was not significant for animals treated with tamoxifen alone (Fig. 5F, Supplementary Fig. S7C). As expected, PolIII and ER phosphorylation were significantly reduced only for the ICEC0942 treatments. Levels of PGR, a well-characterised ER target gene, were greatly reduced in tamoxifen treated tumors ( $p = 0.004$ ), but were also strongly inhibited by ICEC0942 ( $p = 0.023$ ), indicative of inhibition of transcription and/or ER activity by CDK7 inhibition in ER-positive breast cancer cells.

Consistent with earlier observations, animal weights were not different between the treatment arms and there were no evident blood biochemistry differences between the treatment groups, further confirming normal liver and kidney function in the treated animals (Supplementary Fig. S7D-E). Lymphopenia, observed in mice treated with ICEC0942 alone, was not seen

in mice co-treated with tamoxifen at a dose of 50 mg/kg/day ICEC0942 (Supplementary Fig. S7F).

## Discussion

We describe herein the first report of a specific, orally bioavailable non-covalent inhibitor of CDK7. The favourable characteristics of this compound comprise remarkable specificity at the doses used and tumor tissue penetration, combined with sufficient potency to reduce all relevant pharmacodynamic markers examined, including PolII and CDK1/2 phosphorylation, as well as ER phosphorylation. It has excellent characteristics, including aqueous solubility, plasma protein binding as well as absence of hERG liability.

ICEC0942 has acceptable oral bioavailability and moderate clearance, with a large volume of distribution not restricted by PPB, with good tissue penetration, confirmed by analysis of ICEC0942 levels in tumours. Both C<sub>max</sub> and exposure (AUC<sub>t</sub>) increase in a linear manner over a range of 10-100 mg/kg. Over these doses t<sub>max</sub> remains unchanged, indicating no saturation of absorption. ICEC0942 has a few undesirable features such as mild efflux, liver metabolism and inhibition of some CYP genes. However, some drugs with high efflux ratios, such as gefitinib, have been used successfully in patients (38). *In vivo* studies demonstrate a large volume of distribution (tissue penetration) for ICEC0942 and HCT116 xenograft data shows high levels of the compound in the tumor after both single and repeat dosing.

The compound was remarkably well tolerated, with no adverse histological or functional effects on liver or kidney function. Although not directly tested for activity against mouse CDK7, the extremely strong conservation (>90% amino acid identity) between human and murine CDK7, together with their conserved functions in the two species, and ICEC0942-mediated inhibition of PolII phosphorylation in PBMCs, as well as in human cell lines, indicate that ICEC0942 inhibits murine, as well as human CDK7. On this basis, we would expect ICEC0942 to have effects on highly proliferating normal tissues, as indicated by the reduced lymphocyte counts in ICEC0942-treated mice in the xenograft studies. Detailed toxicological studies will be required before progression to the clinic.

Although CDK7 is a ubiquitous kinase that regulates key events in cell cycle progression and transcription, the excellent safety profile of ICEC0942 indicates that the compound exerts preferential inhibitory effects in tumor relative to normal tissue. Interestingly, knockout studies show that although CDK7 is required for embryonic development, it does not appear to be essential for tissues with low proliferation, such as the brain (39). However, CDK7 is important in highly proliferative tissues, such as skin and intestine. Hemizygous deletion of the gene encoding the largest PolII subunit (POLR2A) is frequent in human cancer, POLR2A most commonly being co-deleted with TP53 (40). Increased sensitivity of cancer cells lacking a POL2RA allele to transcription inhibitors implies that many cancers might be highly sensitive to CDK7 inhibition. The fact that transcriptional regulators are important drivers in many cancers types, provides a further explanation for the special sensitivity to inhibitors of transcription, such as CDK7 inhibitors (8-11).

For breast cancer, where ER is the key driver, our results show that ICEC0942 inhibits ER phosphorylation at Ser118, as predicted from prior studies by our group (15). Ser118 phosphorylation is an early event following estrogen binding and is important for cyclical association and dissociation of ER at regulatory regions of target genes that is required for ER-mediated gene expression in breast cancer cells (20,21,41,42). *In vivo*, Ser118 phosphorylation is associated with patient response to endocrine therapies (43), is elevated in endocrine resistant cell lines and in tumors following relapse after tamoxifen treatment (44), highlighting the importance of Ser118 phosphorylation in breast cancer. The importance of Ser118 phosphorylation for ER activity, together with the direct role of CDK7 in transcription, provides a potential explanation for the effectiveness of combining inhibition of ER activity with endocrine agents, together with CDK7 inhibition. Finally, gene expression analysis and IHC have shown that expression of the CDK7 complex (CDK7, cyclin H, MAT1) is elevated in breast tumors compared with the normal breast and is highest in ER-positive, endocrine resistant breast cancer (45), which is further suggestive of cancer selectivity of CDK7 inhibitors.

Several key questions remain before CDK7 inhibition can be considered as a strategy in the treatment of breast cancer. First, although ER is especially susceptible to CDK7 inhibition, presumably other transcription factors contribute to the effects observed. For example, transcriptomic studies for THZ1 have highlighted the special sensitivity of GATA3 expression in AML (8). GATA3 is a marker of luminal breast cancer that is co-expressed with ER and which acts as a pioneer factor promoting ER recruitment to chromatin (46). Indeed, GATA3 expression in MCF7 is as sensitive to THZ1 as is PolII phosphorylation (47). Secondly, the contribution of reduction in CDK1/2/4/6 activities in tumor responses to CDK7 inhibition, remains to be more fully investigated.

THZ1 has a phenylpyrimidine structure with a cysteine-reactive acrylamide moiety, which binds in the ATP binding pocket of CDK7 and covalently links to a cysteine residue, C312, lying outside the ATP pocket, to irreversibly inhibit CDK7 (8). It has potent activity against several cancer types, its reported mode of action being primarily to inhibit PolII activity. However, THZ1 also inhibits the activities of several other kinases, albeit at slightly higher concentrations, for example CDK12 and CDK13, both of which are predicted to be covalently bound by THZ1. Inhibition of these and other kinases, potentially in a covalent manner, may contribute to side effects, although results to date indicate strong cancer cell selectivity over normal cells. Notwithstanding, ICEC0942 is a valuable new selective CDK7 inhibitor with an alternative (non-covalent) mechanism of action and that is orally bioavailable and effective not simply as a single agent but also in combination with endocrine therapies. For ER-positive breast cancer, it will be necessary to establish the timing of CDK7 inhibitor therapy, for example to define whether combining *ab initio* is possible, or if they should be used following emergence of resistance to current therapies. Only well-controlled clinical trials will answer these questions.

## **Acknowledgements**

This work was funded by Cancer Research UK grants C37/A9335, C37/A12011 and C37/A18784 to S.A. C.C and A.G.M.B. Additional support was provided by the Imperial Experimental Cancer Medicine Centre, Imperial NIHR Biomedical Research Centre and the Cancer Research UK Imperial Centre. We thank the Developmental Therapeutics Program at the National Cancer Institute for the NCI60 cancer cell line screening. For expertise on mouse tissue histology and immunohistochemistry, we thank Gordon Stamp and Mahrokh Nohadani. We are particularly grateful to Theo Balasas and Tommy Rennison for help and advice at all stages of this work.

## References

1. Jang MK, Mochizuki K, Zhou M, Jeong HS, Brady JN, Ozato K. The bromodomain protein Brd4 is a positive regulatory component of P-TEFb and stimulates RNA polymerase II-dependent transcription. *Mol Cell* **2005**;19(4):523-34 doi 10.1016/j.molcel.2005.06.027.
2. Yang Z, Yik JH, Chen R, He N, Jang MK, Ozato K, *et al.* Recruitment of P-TEFb for stimulation of transcriptional elongation by the bromodomain protein Brd4. *Mol Cell* **2005**;19(4):535-45 doi 10.1016/j.molcel.2005.06.029.
3. Bisgrove DA, Mahmoudi T, Henklein P, Verdin E. Conserved P-TEFb-interacting domain of BRD4 inhibits HIV transcription. *Proc Natl Acad Sci U S A* **2007**;104(34):13690-5 doi 10.1073/pnas.0705053104.
4. Delmore JE, Issa GC, Lemieux ME, Rahl PB, Shi J, Jacobs HM, *et al.* BET bromodomain inhibition as a therapeutic strategy to target c-Myc. *Cell* **2011**;146(6):904-17 doi 10.1016/j.cell.2011.08.017.
5. Asangani IA, Dommeti VL, Wang X, Malik R, Cieslik M, Yang R, *et al.* Therapeutic targeting of BET bromodomain proteins in castration-resistant prostate cancer. *Nature* **2014**;510(7504):278-82 doi 10.1038/nature13229.
6. Feng Q, Zhang Z, Shea MJ, Creighton CJ, Coarfa C, Hilsenbeck SG, *et al.* An epigenomic approach to therapy for tamoxifen-resistant breast cancer. *Cell Res* **2014**;24(7):809-19 doi 10.1038/cr.2014.71.
7. Ali S, Heathcote DA, Kroll SH, Jogalekar AS, Scheiper B, Patel H, *et al.* The development of a selective cyclin-dependent kinase inhibitor that shows antitumor activity. *Cancer Res* **2009**;69(15):6208-15 doi 10.1158/0008-5472.CAN-09-0301.
8. Kwiatkowski N, Zhang T, Rahl PB, Abraham BJ, Reddy J, Ficarro SB, *et al.* Targeting transcription regulation in cancer with a covalent CDK7 inhibitor. *Nature* **2014**;511(7511):616-20 doi 10.1038/nature13393.
9. Chipumuro E, Marco E, Christensen CL, Kwiatkowski N, Zhang T, Hatheway CM, *et al.* CDK7 inhibition suppresses super-enhancer-linked oncogenic transcription in MYCN-driven cancer. *Cell* **2014**;159(5):1126-39 doi 10.1016/j.cell.2014.10.024.
10. Christensen CL, Kwiatkowski N, Abraham BJ, Carretero J, Al-Shahrour F, Zhang T, *et al.* Targeting Transcriptional Addictions in Small Cell Lung Cancer with a Covalent CDK7 Inhibitor. *Cancer cell* **2014**;26(6):909-22 doi 10.1016/j.ccell.2014.10.019.
11. Wang Y, Zhang T, Kwiatkowski N, Abraham BJ, Lee TI, Xie S, *et al.* CDK7-dependent transcriptional addiction in triple-negative breast cancer. *Cell* **2015**;163(1):174-86 doi 10.1016/j.cell.2015.08.063.
12. Fisher RP. The CDK Network: Linking Cycles of Cell Division and Gene Expression. *Genes Cancer* **2012**;3(11-12):731-8 doi 10.1177/1947601912473308.
13. Bastien J, Adam-Stitah S, Riedl T, Egly JM, Chambon P, Rochette-Egly C. TFIIF interacts with the retinoic acid receptor gamma and phosphorylates its AF-1-activating domain through cdk7. *J Biol Chem* **2000**;275(29):21896-904 doi 10.1074/jbc.M001985200.

14. Rochette-Egly C, Adam S, Rossignol M, Egly JM, Chambon P. Stimulation of RAR alpha activation function AF-1 through binding to the general transcription factor TFIID and phosphorylation by CDK7. *Cell* **1997**;90(1):97-107.
15. Chen D, Riedl T, Washbrook E, Pace PE, Coombes RC, Egly JM, *et al.* Activation of estrogen receptor alpha by S118 phosphorylation involves a ligand-dependent interaction with TFIID and participation of CDK7. *Mol Cell* **2000**;6(1):127-37.
16. Chymkowitz P, Le May N, Charneau P, Compe E, Egly JM. The phosphorylation of the androgen receptor by TFIID directs the ubiquitin/proteasome process. *The EMBO journal* **2011**;30(3):468-79 doi 10.1038/emboj.2010.337.
17. Lee DK, Duan HO, Chang C. From androgen receptor to the general transcription factor TFIID. Identification of cdk activating kinase (CAK) as an androgen receptor NH(2)-terminal associated coactivator. *J Biol Chem* **2000**;275(13):9308-13.
18. Ko LJ, Shieh SY, Chen X, Jayaraman L, Tamai K, Taya Y, *et al.* p53 is phosphorylated by CDK7-cyclin H in a p36MAT1-dependent manner. *Molecular and cellular biology* **1997**;17(12):7220-9.
19. Lu H, Fisher RP, Bailey P, Levine AJ. The CDK7-cycH-p36 complex of transcription factor IID phosphorylates p53, enhancing its sequence-specific DNA binding activity in vitro. *Mol Cell Biol* **1997**;17(10):5923-34.
20. Metivier R, Penot G, Hubner MR, Reid G, Brand H, Kos M, *et al.* Estrogen receptor-alpha directs ordered, cyclical, and combinatorial recruitment of cofactors on a natural target promoter. *Cell* **2003**;115(6):751-63.
21. Reid G, Hubner MR, Metivier R, Brand H, Denger S, Manu D, *et al.* Cyclic, proteasome-mediated turnover of unliganded and liganded ERalpha on responsive promoters is an integral feature of estrogen signaling. *Mol Cell* **2003**;11(3):695-707.
22. Schachter MM, Fisher RP. The CDK-activating kinase Cdk7: taking yes for an answer. *Cell Cycle* **2013**;12(20):3239-40 doi 10.4161/cc.26355.
23. Schachter MM, Merrick KA, Larochelle S, Hirschi A, Zhang C, Shokat KM, *et al.* A Cdk7-Cdk4 T-loop phosphorylation cascade promotes G1 progression. *Mol Cell* **2013**;50(2):250-60 doi 10.1016/j.molcel.2013.04.003.
24. Malumbres M, Barbacid M. Cell cycle, CDKs and cancer: a changing paradigm. *Nat Rev Cancer* **2009**;9(3):153-66 doi 10.1038/nrc2602.
25. Finn RS, Crown JP, Lang I, Boer K, Bondarenko IM, Kulyk SO, *et al.* The cyclin-dependent kinase 4/6 inhibitor palbociclib in combination with letrozole versus letrozole alone as first-line treatment of oestrogen receptor-positive, HER2-negative, advanced breast cancer (PALOMA-1/TRIO-18): a randomised phase 2 study. *The lancet oncology* **2015**;16(1):25-35 doi 10.1016/S1470-2045(14)71159-3.
26. Turner NC, Huang Bartlett C, Cristofanilli M. Palbociclib in Hormone-Receptor-Positive Advanced Breast Cancer. *N Engl J Med* **2015**;373(17):1672-3 doi 10.1056/NEJMc1510345.
27. Heathcote DA, Patel H, Kroll SH, Hazel P, Periyasamy M, Alikian M, *et al.* A novel pyrazolo[1,5-a]pyrimidine is a potent inhibitor of cyclin-



- dependent protein kinases 1, 2, and 9, which demonstrates antitumor effects in human tumor xenografts following oral administration. *Journal of medicinal chemistry* **2010**;53(24):8508-22 doi 10.1021/jm100732t.
28. Bondke A, Kroll S, Barrett A, Fuchter M, Slafer B, Ali S, *et al.*; Imperial Innovations Ltd, Cancer Research Technology Ltd, Emory University, assignee. Pyrazolo[1,5-A]pyrimidine-5,7-diamine compounds as CDK inhibitors and their therapeutic use. US patent 0362410 A1. 2016.
  29. Capes-Davis A, Reid YA, Kline MC, Storts DR, Strauss E, Dirks WG, *et al.* Match criteria for human cell line authentication: where do we draw the line? *International journal of cancer Journal international du cancer* **2013**;132(11):2510-9 doi 10.1002/ijc.27931.
  30. Skehan P, Storeng R, Scudiero D, Monks A, McMahon J, Vistica D, *et al.* New colorimetric cytotoxicity assay for anticancer-drug screening. *J Natl Cancer Inst* **1990**;82(13):1107-12.
  31. Workman P, Aboagye EO, Balkwill F, Balmain A, Bruder G, Chaplin DJ, *et al.* Guidelines for the welfare and use of animals in cancer research. *British journal of cancer* **2010**;102(11):1555-77 doi 10.1038/sj.bjc.6605642.
  32. Rubin SM. Deciphering the retinoblastoma protein phosphorylation code. *Trends in biochemical sciences* **2013**;38(1):12-9 doi 10.1016/j.tibs.2012.10.007.
  33. Laroche S, Merrick KA, Terret ME, Wohlbold L, Barboza NM, Zhang C, *et al.* Requirements for Cdk7 in the assembly of Cdk1/cyclin B and activation of Cdk2 revealed by chemical genetics in human cells. *Mol Cell* **2007**;25(6):839-50 doi 10.1016/j.molcel.2007.02.003.
  34. Zannini L, Delia D, Buscemi G. CHK2 kinase in the DNA damage response and beyond. *J Mol Cell Biol* **2014**;6(6):442-57 doi 10.1093/jmcb/mju045.
  35. Anderson VE, Walton MI, Eve PD, Boxall KJ, Antoni L, Caldwell JJ, *et al.* CCT241533 is a potent and selective inhibitor of CHK2 that potentiates the cytotoxicity of PARP inhibitors. *Cancer Res* **2011**;71(2):463-72 doi 10.1158/0008-5472.CAN-10-1252.
  36. Lannigan DA. Estrogen receptor phosphorylation. *Steroids* **2003**;68(1):1-9.
  37. Brodie A, Jelovac D, Macedo L, Sabnis G, Tilghman S, Goloubeva O. Therapeutic observations in MCF-7 aromatase xenografts. *Clinical cancer research : an official journal of the American Association for Cancer Research* **2005**;11(2 Pt 2):884s-8s.
  38. Agarwal S, Sane R, Gallardo JL, Ohlfest JR, Elmquist WF. Distribution of gefitinib to the brain is limited by P-glycoprotein (ABCB1) and breast cancer resistance protein (ABCG2)-mediated active efflux. *J Pharmacol Exp Ther* **2010**;334(1):147-55 doi 10.1124/jpet.110.167601.
  39. Ganuza M, Saiz-Ladera C, Canamero M, Gomez G, Schneider R, Blasco MA, *et al.* Genetic inactivation of Cdk7 leads to cell cycle arrest and induces premature aging due to adult stem cell exhaustion. *EMBO J* **2012**;31(11):2498-510 doi 10.1038/emboj.2012.94.
  40. Liu Y, Zhang X, Han C, Wan G, Huang X, Ivan C, *et al.* TP53 loss creates therapeutic vulnerability in colorectal cancer. *Nature* **2015**;520(7549):697-701 doi 10.1038/nature14418.

41. Metivier R, Reid G, Gannon F. Transcription in four dimensions: nuclear receptor-directed initiation of gene expression. *EMBO reports* **2006**;7(2):161-7 doi 10.1038/sj.embor.7400626.
42. Valley CC, Metivier R, Solodin NM, Fowler AM, Mashek MT, Hill L, *et al.* Differential regulation of estrogen-inducible proteolysis and transcription by the estrogen receptor alpha N terminus. *Mol Cell Biol* **2005**;25(13):5417-28 doi 10.1128/MCB.25.13.5417-5428.2005.
43. Skliris GP, Nugent ZJ, Rowan BG, Penner CR, Watson PH, Murphy LC. A phosphorylation code for oestrogen receptor-alpha predicts clinical outcome to endocrine therapy in breast cancer. *Endocrine-related cancer* **2010**;17(3):589-97 doi 10.1677/ERC-10-0030.
44. Sarwar N, Kim JS, Jiang J, Peston D, Sinnott HD, Madden P, *et al.* Phosphorylation of ERalpha at serine 118 in primary breast cancer and in tamoxifen-resistant tumours is indicative of a complex role for ERalpha phosphorylation in breast cancer progression. *Endocrine-related cancer* **2006**;13(3):851-61 doi 10.1677/erc.1.01123.
45. Patel H, Abduljabbar R, Lai CF, Periyasamy M, Harrod A, Gemma C, *et al.* Expression of CDK7, Cyclin H, and MAT1 Is Elevated in Breast Cancer and Is Prognostic in Estrogen Receptor-Positive Breast Cancer. *Clinical cancer research : an official journal of the American Association for Cancer Research* **2016** doi 10.1158/1078-0432.CCR-15-1104.
46. Theodorou V, Stark R, Menon S, Carroll JS. GATA3 acts upstream of FOXA1 in mediating ESR1 binding by shaping enhancer accessibility. *Genome research* **2013**;23(1):12-22 doi 10.1101/gr.139469.112.
47. Harrod A, Fulton J, Nguyen VT, Periyasamy M, Ramos-Garcia L, Lai CF, *et al.* Genomic modelling of the ESR1 Y537S mutation for evaluating function and new therapeutic approaches for metastatic breast cancer. *Oncogene* **2016** doi 10.1038/onc.2016.382.

## Figure legends

**Figure 1.** ICEC0942 is a CDK7 selective inhibitor of cancer cell growth. *A*, Compound structure of ICEC0942. *B*, *In vitro* kinase assays. Inhibition of kinase activity is shown relative to the vehicle treatment, as the mean of 3 experiments; errors bars show SEM. *C*, Cell lines were treated with increasing concentrations of ICEC0942 for 48 hours. GI<sub>50</sub> values are shown for three independent experiments. *D*, Box and whisker plot (5-95 percentile) showing that ICEC0942 inhibits proliferation of the NCI panel of 60 cancer cell lines. The black dots show cancer cell lines for which GI<sub>50</sub> values were outside the 5-95 percentile.

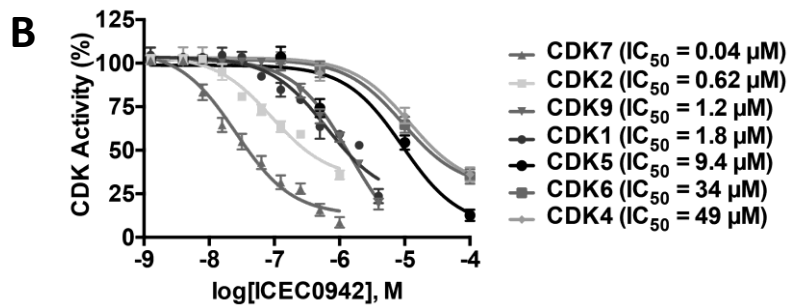
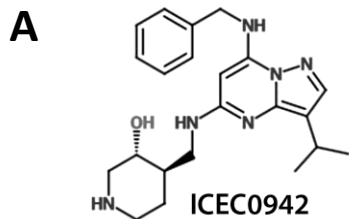
Figure 2. ICEC0942 inhibits phosphorylation of CDK7 substrates, to promote cell cycle arrest and apoptosis. *A*, HCT116 cells were treated with ICEC0942 at concentrations shown. Cell lysates were prepared at the indicated time points following ICEC0942 addition. *B*, Percentage of apoptotic HCT116 cells 24 hours following addition of ICEC0942, determined by Annexin V and propidium iodide staining (n=3 independent experiments; \* = p<0.05 relative to vehicle (0) control); t-test. *C-D*, Cell lysates, prepared 24 hours following addition of ICEC0942 were immunoblotted for PARP cleavage or assayed for caspase 3/7 activity (n=3). *E*, Flow cytometric analysis was carried out for HCT116 cells 24 hours following addition of ICEC0942 at concentrations shown. Mean percentage of cells in G1, S and G2/M phases are shown for three independent experiments; error bars depict SEM, \* = statistically significant (p<0.05) difference between percentage of cells in G1 compared with the vehicle control, # = statistically significant (p<0.05) difference between percentage of cells in G2/M, compared with the vehicle control. *F*, MCF7 cells were arrested in G0/G1, S-phase, or in G2/M. Cells were released from the block by washing and replenishment with fresh medium supplemented with ICEC0942. Shown are the FACS profiles 24 hours following addition of ICEC0942. The numbers below each graph are the percentage of cells in G1, S-phase or G2/M for each enrichment condition for one experiment. These data are included in the time course in Supplementary Figure S3A.

**Figure 3.** Inhibition of MCF7 tumour xenografts by ICEC0942 is accompanied by reduction in phosphorylation of CDK7 substrates. *A*, Mean tumor volumes  $\pm$ SEM, for randomized nude mice bearing MCF7 tumors treated with 100 mg/kg/day ICEC0942 (n=12 in each arm). Linear regression showed statistically significant ( $p<0.0001$ ) difference in growth between vehicle and ICEC0942 treated animals. *B*, FACS of immunostained PBMCs, collected 6 hours after ICEC0942 administration (n=3;  $*=p<0.05$ ; t-test). *C*, Immunostaining for PolII, or phosphorylated PolII (1,000 cells/tumor) from vehicle or ICEC0942 treated animals. Representative IHC images are shown. *D*, Immunoblotting of protein lysates prepared from 3 tumors.

**Figure 4.** ICEC0942 inhibits growth of colon cancer tumor xenografts. *A-B*, Nude mice bearing HCT116 tumors were randomized for PO treatment with 100 mg/kg/daily ICEC0942. Mean tumour volumes  $\pm$ SEM and mouse weights are shown (n=15). Linear regression analysis showed statistically significant ( $p<0.0001$ ) difference in growth between vehicle and ICEC0942 treated animals. *C*, Immunostaining of resected tumors for PolII and PolIII Ser2 and Ser5 phosphorylation. Graphed are the scoring of 1000 cells for 3 tumors in each group. *D*, Immunostaining of PBMCs collected at the end of the study (n=3;  $*=p<0.05$ ; t-test). *E*, Biochemistry of bloods collected 6 hours after first or last administration (n=3). *F*, Blood cell analysis at day 13 of ICEC0942 or vehicle treatment. Also shown are blood counts for animals bearing HCT116 tumors ranging in size from 100-200 mm<sup>3</sup> (n=6) and for 3 nude mice without tumors or treatment.

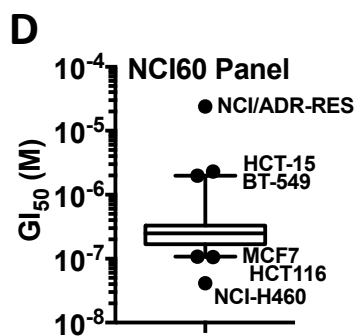
**Figure 5.** Co-operativity between the CDK7 inhibitor ICEC0942 and hormone therapies *in vitro* and *in vivo*. *A*, MCF7 cells were treated with ICEC0942 in the presence or absence of the anti-estrogens Tamoxifen or Faslodex over a 12 day period. Growth is shown relative to the vehicle control (n=3). Asterisks represent significant difference ( $p<0.05$ ) in growth relative to cells grown in the absence of ICEC0942. The hash symbol (#) shows significant ( $p<0.05$ ) difference in growth between cells cultured in the presence of anti-estrogen and 0.1  $\mu$ M ICEC0942, compared with cells cultured only in the presence of

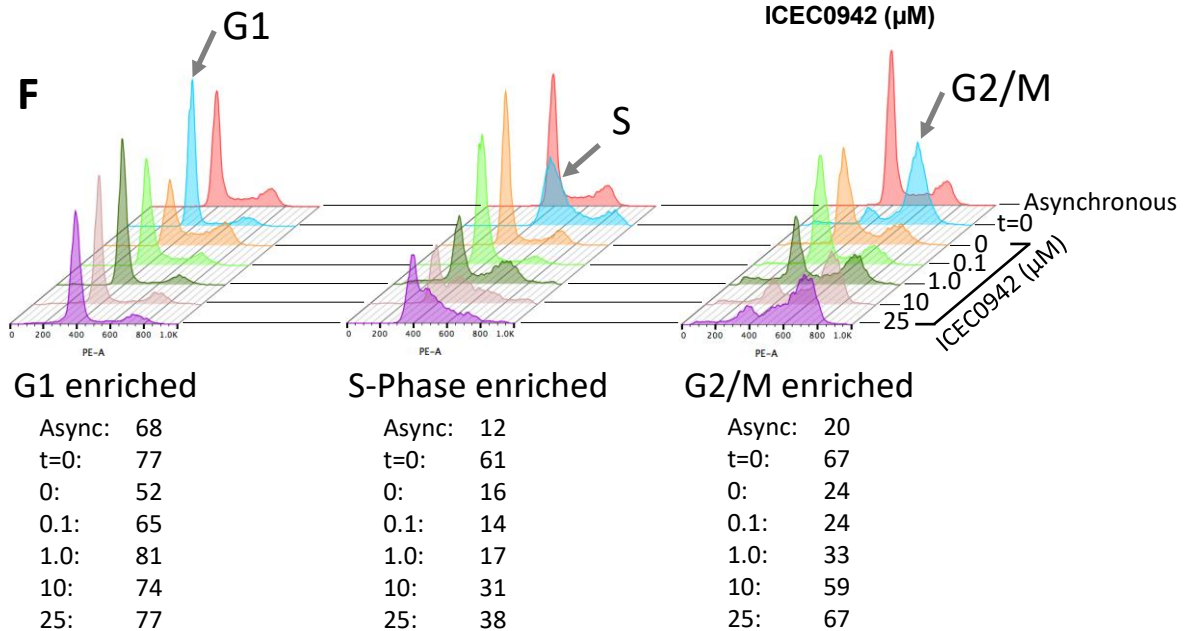
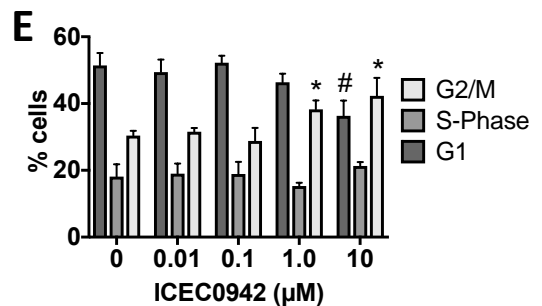
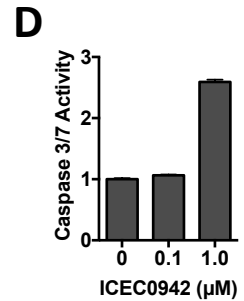
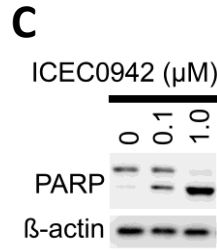
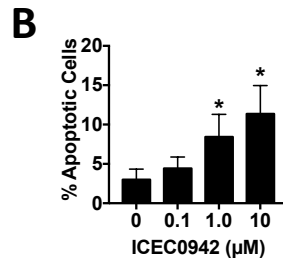
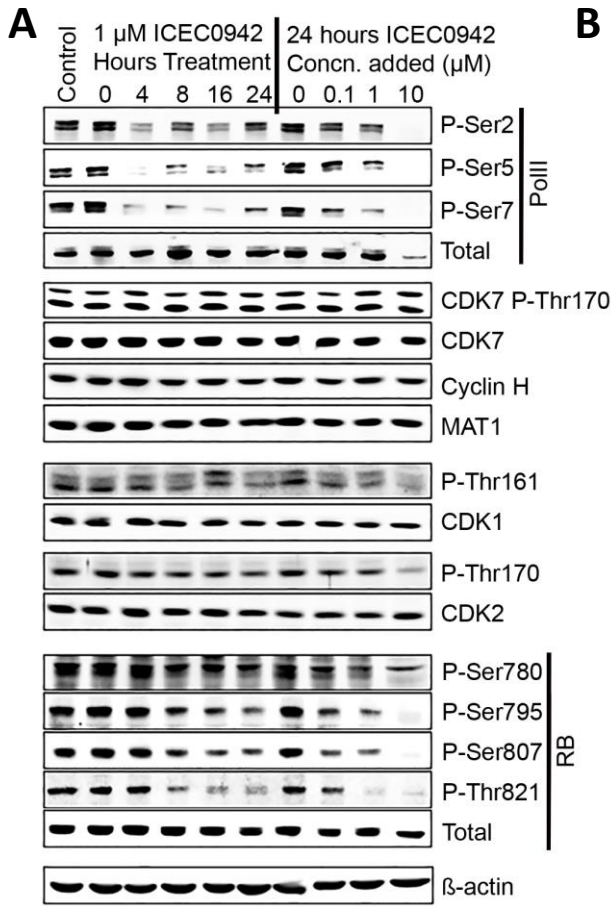
0.1  $\mu$ M ICEC0942. *B*, Immunoblotting was performed for MCF7 cells treated for 24 hours, with ICEC0942 and/or tamoxifen at the concentrations shown. *C*, Flow cytometric analysis was carried out for MCF7 cells 24 hours following addition of ICEC0942 and/or tamoxifen, at concentrations shown. Mean percentage of cells in G1, S and G2/M phases are shown for three independent experiments; error bars depict SEM, \* = statistically significant ( $p < 0.05$ ) difference between percentage of cells in G2/M compared with the vehicle control, # = statistically significant ( $p < 0.05$ ) difference between percentage of cells in G1, compared with the vehicle control. *D*, Percentage of apoptotic MCF7 cells 24 hours following addition of ICEC0942 and/or tamoxifen, determined by Annexin V and propidium iodide staining ( $n = 3$  independent experiments; \* =  $p < 0.05$  relative to vehicle (0) control); t-test. *E*, Animals with MCF7 tumor xenografts treated once daily with vehicle, 100  $\mu$ g tamoxifen and/or 50 mg/kg ICEC0942 ( $n = 8$  for each arm of the study). Multiple comparison test using one-way ANOVA analysis of slopes of linear regression lines was statistically significant ( $p = 0.0002$ ) for the different treatment groups. Shown are the adjusted  $p$ -values for treatment pairs from the multiple comparison testing. *F*, IHC was performed for tumors from 3 animals and scoring done as for Fig. 3. Asterisks show significant differences ( $p < 0.05$ ) from the vehicle treated tumors. All statistical analyses were undertaken using the t-test.

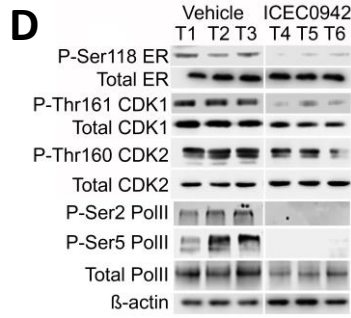
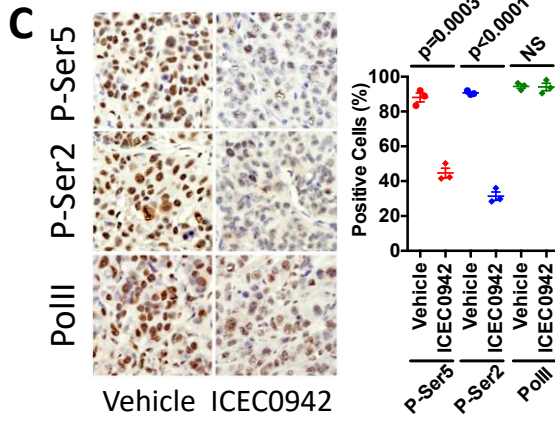
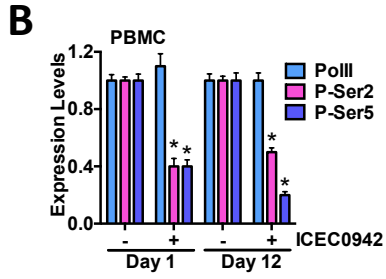
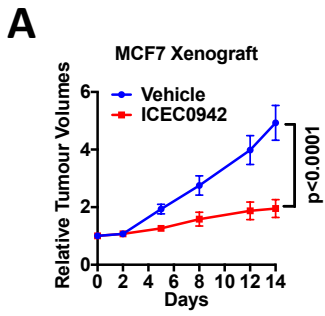


**C**

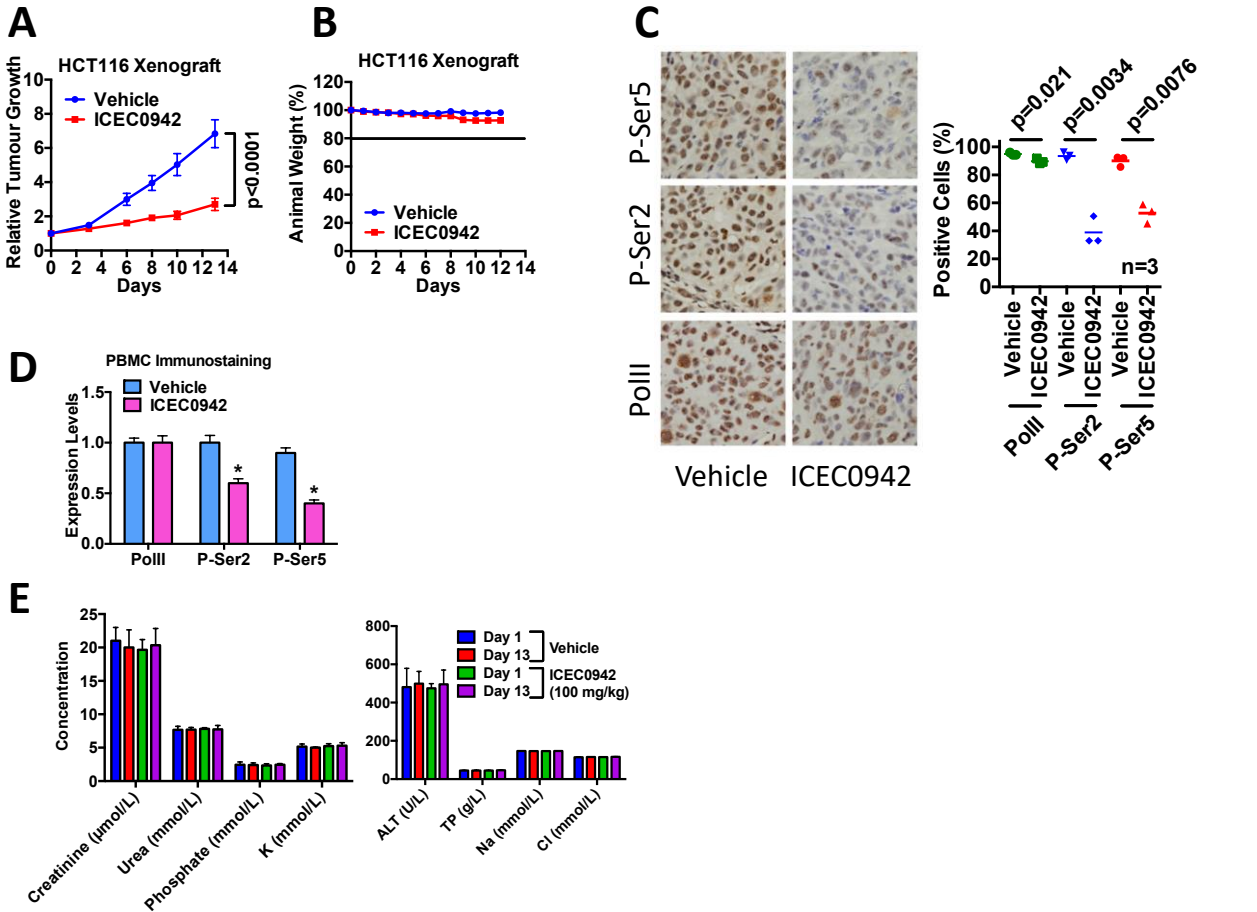
Cell Line	ICEC0942 [ $GI_{50}$ ( $\mu\text{M}$ )]
MCF7	0.18
T47D	0.32
MDA-MB-231	0.33
HS578T	0.21
MDA-MB-468	0.22
MCF10A	0.67
HMEC	1.25











**F**

	units	Control mice Range (n=3)	Tumor bearing mice Range (n=6)	Vehicle (n=3)		100mg/kg/day (n=3)	
				Average	SEM	Average	SEM
Red blood cell	$10^{12}/L$	8.90-9.07	8.37-9.0	8.3	0.3	8.5	0.1
Hemoglobin	g/dl	14.7-15.4	14.1-15.3	14.0	0.3	14.2	0.3
Hematocrit	L/L	0.519-0.526	0.461-0.515	0.5	0.0	0.5	0.0
Mean corpuscular volume	fL	57.0-58.1	55-57	55.0	0.6	55.7	0.9
Mean corpuscular hemoglobin	pg	16.6-17.0	16.3-17.0	16.9	0.2	16.6	0.2
Mean corpuscular hemoglobin concentration	g/dL	28.0-29.1	29.3-30.9	30.8	0.5	30.0	1.0
Red cell distribution width		15.5-16.5	16.3-18	17.3	0.4	17.0	0.4
Platelet	$10^9/L$	333-614	582-1097	722.0	53.4	757.0	59.2
Mean platelet volume	fL	6.9-7.9	6.2-8.1	7.5	0.5	7.6	0.3
White blood cells	$10^9/L$	1.7-6.5	6.9-9.5	9.5	0.3	4.0	0.7
Neutrophils	$10^9/L$	0.9-2.7	0.6-3.3	3.3	0.1	1.1	0.2
Lymphocytes	$10^9/L$	0.8-1.7	5.7-6.6	6.1	0.2	1.1	0.5
Monocytes	$10^9/L$	0.0-0.1	0.1-0.3	0.1	0.1	0.1	0.0
Eosinophils	$10^9/L$	0.0	0.0	0.0	0.0	0.0	0.0
Basophils	$10^9/L$	0.0	0-0.1	0.0	0.0	1.7	0.2

